Hole mobility of GaAs, GaP, and $GaAs_{1-x}P_x$ mixed-compound semiconductors

Kyozaburo Takeda and Nobuo Matsumoto
Musashino Electrical Communication Laboratory, Nippon Telegraph and Telephone Public Corporation, Musashino-shi, Tokyo 180, Japan

Akihito Taguchi,* Hiroyuki Taki, Eiji Ohta, and Makoto Sakata
Department of Instrumentation Engineering, Faculty of Science and Technology, Keio University, Yokohama 223, Japan
(Received 16 May 1984; revised manuscript received 29 October 1984)

With the use of the substitutional virtual-crystal-approximation method, the composition dependence is semiempirically estimated for the $GaAs_{1-x}P_x$ valence-band parameter and the hole-phonon coupling constants. Alloy scattering is also investigated with the help of dielectric band theory. Taking account of the inter-valence-band interaction, we discuss theoretical hole mobility using two different approaches: the conventional effective-relaxation-time approximation and Rode's difference approximation. Owing to decreased split-off energy, the influence of inter-valence-band interaction on the hole material parameter is strengthened with increased P content and temperature.

I. INTRODUCTION

Many experimental results from structural analysis indicate that III-V mixed-alloy compounds are substitutional ones, in which impurity atoms of group III replace themselves at the positions of host atoms of group III, and not at the positions of group-V atoms, and vice versa.[1] This means that III-V mixed-alloy compounds do not belong to "strict" zinc-blende crystals of T_d representation. Accordingly, the results of the $\mathbf{k}\cdot\mathbf{p}$ band calculation developed by Dresselhaus, Kip, and Kittel[2] (DKK) and Kane[3] for zinc-blende structure cannot be applied in a straightforward manner.

With replacement of atoms in the sublattice of diamond structure by different atoms, a zinc-blende structure is produced. Further ordered replacement in the zinc-blende structure, such as a group-III element alternatively substituted by a different group-III element (e.g., the GaAs GaP GaAs... stacked structure of $GaAs_{0.5}P_{0.5}$, an "ordered mixed alloy"), changes the space group from T_d to D_{2d}. Thus, the term K (Ref. 3) resulting from a lack of inversion symmetry in zinc-blende structure is thought to be a "randomness" term for each particular case of atomic replacement. In order to be able to discuss substitutional randomness in mixed alloys, it is necessary to consider the absence of spatial symmetries due to alloying. K values are, however, very small, even with a change from elementary semiconductors to compound semiconductors, which introduces a virtual zinc-blende crystal structure for III-V mixed alloys. In this paper we use, therefore, a "substitutional virtual-crystal approximation" (SVCA) in which the same-group atoms replace themselves at the same-group atomic sites.

Only a few theoretical analyses of hole-transport coefficients for mixed-compound semiconductors have been reported,[4] in which the treatment of the existence of three types of holes (heavy, light, and split-off holes) and inter-valence-band interactions is not sufficiently developed. Experimental investigations of fundamental hole parameters for Ga-As-P alloys have rarely been reported. Thus, we obtained the valence-band parameter semiempirically, and determined the band structure near the valence-band edge (Sec. II).[5] Next, hole-phonon coupling constants were estimated and the scattering rates for several processes were calculated.[5] Alloy scattering was also considered (Sec. III).[5] By solving a coupled Boltzmann equation, hole-transport coefficients (mobility) were obtained (Sec. IV). We also investigated the composition dependence of the above-mentioned hole parameters, paying attention to the inter-valence-band interaction and how the three types of holes come into play.

The following theoretical calculation method will be applicable to those 18 ternary alloys produced by a combination of group-III (Al,Ga,In) and group-V (P,As,Sb) elements. However, experimental material parameters of those ternary alloys have hardly been reported. $GaAs_{1-x}P_x$ is one ternary alloy whose experimental data are comparatively well reported in III-V ternary mixed compounds. Therefore, this paper presents the calculated results of $GaAs_{1-x}P_x$ in order to compare our calculated results with previous experimental results.

II. BAND STRUCTURE

A. ϵ-$\mathbf{k}$ dispersion relation

The energy-band structure near the valence-band edge of III-V compounds has been investigated in the past using second-order $\mathbf{k}\cdot\mathbf{p}$ perturbation theory, including spin-orbit interaction.[2,3] The resulting valence band consists of three sub-valence-bands (heavy, light, and split-off holes). Spin-orbit interaction partially removes degeneracy by lowering the two bands with $J=\frac{1}{2}$ to four bands with $J=\frac{3}{2}$. The former two bands ($J=\frac{1}{2}$) are known as the split-off hole bands, and the latter four ($J=\frac{3}{2}$) as heavy- and light-hole bands, respectively. In order to obtain energy eigenvalues by the $\mathbf{k}\cdot\mathbf{p}$ approach, it is necessary to solve the following 6×6 secular equation (Kane model)

$$
\begin{vmatrix}
\frac{H_{11}+H_{22}}{2}-\epsilon+\frac{\hbar^2}{2m}k^2 & -\frac{H_{13}-iH_{23}}{\sqrt{3}} & -\frac{H_{11}-H_{22}-2iH_{12}}{2\sqrt{3}} & 0 & -\frac{H_{13}-iH_{23}}{\sqrt{6}} & -\frac{H_{11}-H_{22}-2iH_{12}}{\sqrt{6}} \\
-\frac{H_{13}+iH_{23}}{\sqrt{3}} & \frac{4H_{33}+H_{11}+H_{22}}{6}-\epsilon+\frac{\hbar^2}{2m}k^2 & 0 & -\frac{H_{11}-H_{22}-2iH_{12}}{2\sqrt{3}} & -\frac{H_{11}+H_{22}-2H_{33}}{3\sqrt{2}} & -\frac{H_{13}+iH_{23}}{\sqrt{2}} \\
-\frac{H_{11}-H_{22}+2iH_{12}}{2\sqrt{3}} & 0 & \frac{4H_{33}+H_{11}+H_{22}}{6}-\epsilon+\frac{\hbar^2}{2m}k^2 & \frac{H_{13}+iH_{23}}{\sqrt{3}} & \frac{H_{13}-iH_{23}}{\sqrt{2}} & \frac{H_{11}+H_{22}-2H_{33}}{3\sqrt{2}} \\
0 & -\frac{H_{11}-H_{22}+2iH_{12}}{2\sqrt{3}} & \frac{H_{13}-iH_{23}}{\sqrt{3}} & \frac{H_{11}+H_{22}}{2}-\epsilon+\frac{\hbar^2}{2m}k^2 & \frac{H_{11}-H_{22}-2iH_{12}}{\sqrt{6}} & -\frac{H_{13}-iH_{23}}{\sqrt{6}} \\
-\frac{H_{13}+iH_{23}}{\sqrt{6}} & -\frac{H_{11}+H_{22}-2H_{33}}{3\sqrt{2}} & \frac{H_{13}-iH_{23}}{\sqrt{2}} & \frac{H_{11}-H_{22}+2iH_{12}}{\sqrt{6}} & \frac{H_{11}+H_{22}+H_{33}}{3}-\epsilon+\frac{\hbar^2}{2m}k^2-\Delta_0 & 0 \\
-\frac{H_{11}-H_{22}+2iH_{12}}{\sqrt{6}} & \frac{H_{13}+iH_{23}}{\sqrt{2}} & \frac{H_{11}+H_{22}-2H_{33}}{3\sqrt{2}} & -\frac{H_{13}+iH_{23}}{\sqrt{6}} & 0 & \frac{H_{11}+H_{22}+H_{33}}{3}-\epsilon+\frac{\hbar^2}{2m}k^2-\Delta_0
\end{vmatrix}
=0. \quad (1)
$$

(as shown at left): Matrix elements H_{ij} are from Dresselhaus *et al.*[2] and Kane.[3]

The interaction between the $J=\frac{3}{2}$ bands and $J=\frac{1}{2}$ band (called an inter-valence-band interaction) affects the roots to order k^4/Δ_0, where Δ_0 is the split-off energy. When the value of k^4/Δ_0 is small, a comprehensive ϵ-k dispersion relation (DKK model) can be introduced neglecting the inter-valence-band interaction, and the problem is reduced to solving two decomposed, small 4×4 and 2×2 matrices. This assumption is only proper, however, at the top of the valence band and for materials with a larger energy. The inter-valence-band interaction warps the energy-band structure and produces nonparabolicity in the ϵ-k relation. The existence of this interaction and the three types of holes have a remarkable effect on scattering mechanisms and transport phenomena for holes.[6]

The symmetry at the top of the valence band is that given by the bonding p-type functions in a tight-binding picture, namely, Γ_{15} in a zinc-blende structure. The lack of spatial symmetry for this type of lattice allows terms of the form $\langle x \mid P_z \mid z \rangle$, which produces a characteristic k-linear term for III-V compounds.[3] The interaction matrix $\hat{H}_{\text{lin}}$, for these terms was shown by Dresselhaus[7] to be of the form[3]

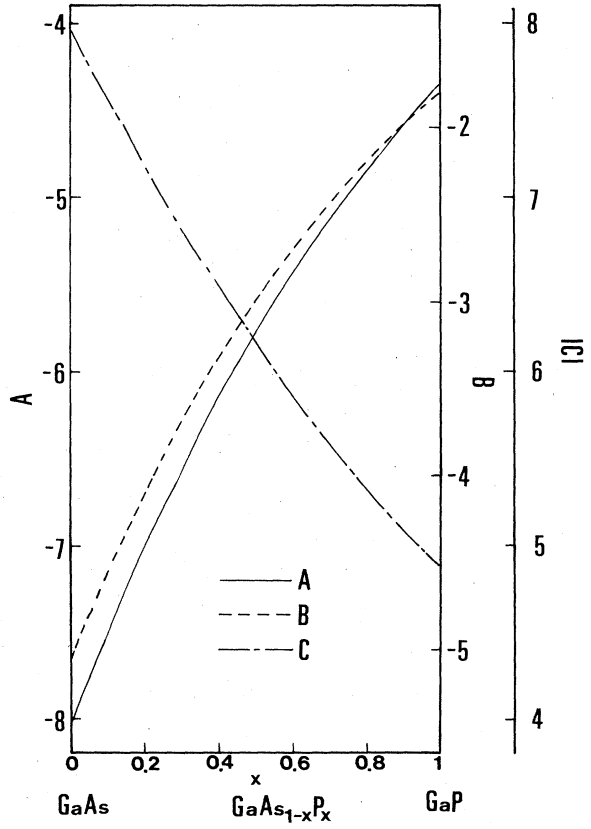

FIG. 1. Resulting valence-band parameters A, B, and C for Ga-As-P alloy system. All the values are given in atomic units.

$$\hat{H}_{\text{lin}} = -\frac{K}{2}\begin{vmatrix} 0 & k_x+ik_y & -2k_z & \sqrt{3}(k_x-ik_y) \\ k_x-ik_y & 0 & \sqrt{3}(k_x+ik_y) & 2k_z \\ -2k_z & -\sqrt{3}(k_x-ik_y) & 0 & k_x+ik_y \\ \sqrt{3}(k_x+ik_y) & 2k_z & k_x-ik_y & 0 \end{vmatrix} . \quad (2)$$

The constant K is a result of the three types of contributions.[3] The following approximate formulas of the k-linear term for heavy and light holes have been given:

$$\epsilon_H^{\text{lin}} = \pm 3\sqrt{3}Kk\sqrt{\lambda}, \quad \epsilon_L^{\text{lin}} = \pm 3\sqrt{3}Kk\sqrt{\lambda - 8\nu},$$

where

$$\lambda = \sin^2\theta(\sin^2\theta\sin^2\phi + \cos^2\theta)(\cos^2\theta + \sin^2\theta\cos^2\phi) ,$$
$$\nu = \sin^4\theta\cos^2\theta\cos^2\phi\sin^2\phi . \quad (3)$$

Here spherical coordinates are used.

By combining the above representations for k-linear terms with the two types of solutions[8] for the secular equation (1) we can introduce two different band models for the DKK and Kane scheme. The inter-valence-band interaction is then investigated by comparing these two band models in tandem.[6,9]

B. Band parameters and effective mass

Valence-band parameters A, B, C, and K are necessary to describe numerically the energy-band structure when the $\mathbf{k}\cdot\mathbf{p}$ method is employed. Under the SVCA assumption, the parameters for ternary mixed alloys of $GaAs_{1-x}P_x$ can be estimated by extending Lawaetz's scaling approach.[10] We consider here the alloying effect as producing a change in the nearest-neighbor distance.

Thompson, Cardona, Shaklee, and Wooley[11] (TCSW) measured the electroreflectance spectra series of $GaAs_{1-x}P_x$ alloys at room temperature. Using their results, we have determined that several direct energy gaps appear in the second-order $\mathbf{k}\cdot\mathbf{p}$ interaction terms (F, G, H_1, and H_2). TCSW reported the variation of E_0, E_1, E_0', and E_2 peaks with P concentration, and also gave empirical expressions for variations in these values with concentration. Symbols E_0, E_1, E_0', and E_2 represent the direct energy gap between Γ_{15}^v and Γ_1^c, L_3^v and L_1^c, Γ_{15}^v and Γ_{12}^c, and X_5^v and X_1^c, respectively.

The direct energy gap can be also semiempirically estimated from the Phillips–Van Vechten[12,13] dielectric band theory.[5] Those semiempirical values[5] are, however, different from TCSW's experimental results. Phillips and Van Vechten have fitted values for all of the III-V compounds so as to obtain a universal factor that systematically describes values for each individual compound. Therefore, numerical ambiguity is caused, for example, in the superscript of lattice constants and in the adjusting parameter for the heteropolar energy (e.g., unity from Van Vechten[13] and 1.25 from Lawaetz[10]). This is one reason for the discrepancy between TCSW experimental results and semiempirical results of the dielectric band theory. We have used the TCSW results to estimate the valence-band parameters for $GaAs_{1-x}P_x$ alloy systems to avoid such ambiguity.

The small difference in effective charge density, N_{eff} between GaAs (4.9) and GaP (4.4) introduces the possibility of linear interpolation for the enhancement factor[10] D of $GaAs_{1-x}P_x$ alloys. Similar linear interpolation can be applied to parameter K because of SVCA. The resulting DKK valence-band parameters (A, B, and C) with use of these fundamental values are shown in Fig. 1. Considerable "bowing" can be found in these parameters.

As the DKK band structure is basically parabolic, the effective masses are independent of energy. On the other hand, the Kane band structure is nonparabolic, which brings about energy-dependent effective masses. By thermally averaging (Eq. 4), with a hole distribution function, the temperature dependence of hole effective masses can be investigated:

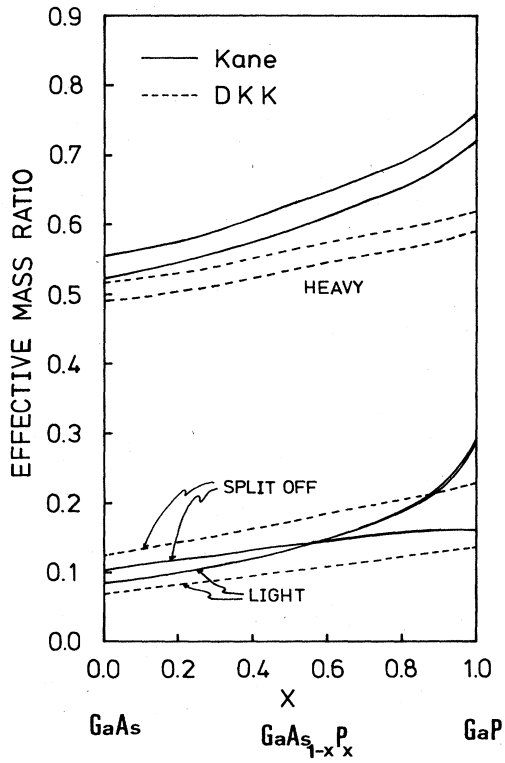

FIG. 2. Composition dependence of hole effective masses (heavy, light, and split-off holes) for Ga-As-P at 300 K. Values represented by solid curves are calculated using the Kane band model in Eq. (4), dashed-curve values using the Dresselhaus, Kip, and Kittel (DKK) band model.

$$\frac{m^*(T)}{m_0} = \int [m^*(k)/m_0]k^2 f_k d\Omega\, dk \Big/ \int f_k k^2 d\Omega\, dk,$$

where

$$\frac{m^*(k)}{m_0} = \frac{k}{2\pi} \int \frac{d\Omega}{|\nabla_k \epsilon_k|} \tag{4}$$

(in atomic units).

Figure 2 shows the resulting composition dependence of effective mass for $GaAs_{1-x}P_x$ alloys at 300 K. The effect of the k-linear term can be found most strongly in the spin separation of heavy-hole bands, though it can hardly be seen in light-hole bands. The inter-valence-band interaction promotes an increase in effective mass for heavy and light holes but a decrease for split-off holes. This effect is strengthened with an increase in P content because the decrease in split-off energy produced a strong nonparabolic and warped valence band in P-rich $GaAs_{1-x}P_x$ alloys. The change in composition dependence near $x=0.7$ is caused by a change of the conduction-band structure from a direct (GaAs) to an indirect (GaP) type.[14]

III. SCATTERING MECHANISMS AND RELAXATION TIMES

A. Lattice scattering

In the present work, four kinds of lattice scattering processes have been taken into account: acoustic-mode deformation-potential scattering (AC), nonpolar optic-phonon scattering (NPO), polar optic-phonon scattering (PO), and piezoelectric scattering (PZ). Since those hole-phonon coupling constants had not been clarified either experimentally or theoretically for Ga-As-P, we first proceeded to estimate these values semiempirically by extending the results of Keyes[15] and using Lawaetz-Wiley expressions,[16] before investigating the relaxation time.

Keyes[15] found empirically that reduced elastic constants, C_u^* ($u=11$, 12, and 14), have nearly unique values within the same group of group-IV, -III-V, and -II-VI semiconductors. The values of the reduced elastic constant C_u^* for GaAs and GaP are shown in Table I. Keyes defined the fundamental elastic constant using the elementary electronic charge q. This produces, however, a slight ambiguity in C_u^* between GaAs and GaP (Table I) because of differences of heteropolarity for constituent elements Ga, As, and P. To avoid this ambiguity, we introduce here the averaged reduced elastic constant $\langle C_u^* \rangle$. The alloying, incorporated by means of a change in nearest-neighbor bond lengths, produces bowing in the elastic constants.

TABLE I. Keyes's reduced elastic constants C_u^* ($u=11,12,$ and 44) for GaAs and GaP, and those averaged values $\langle C_u^* \rangle$.

	Averaged reduced elastic constant	Keyes's reduced elastic constant	
		GaP	GaAs
$\langle C_{11}^* \rangle$	1.821	1.898	1.848
$\langle C_{12}^* \rangle$	0.912	0.841	0.837
$\langle C_{44}^* \rangle$	0.879	0.947	0.924

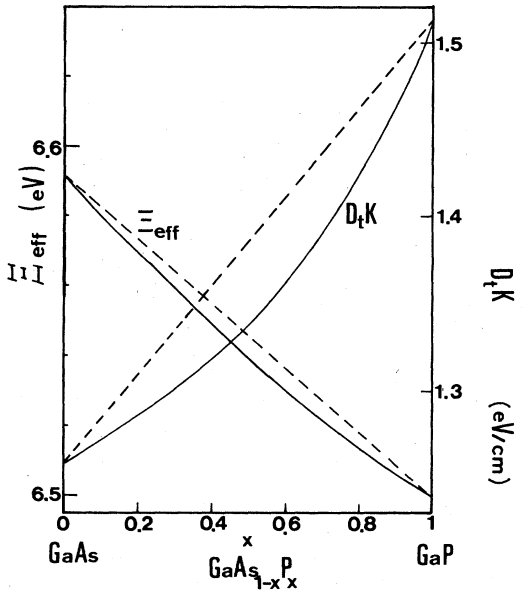

FIG. 3. Calculated acoustic-mode effective deformation potential Ξ_{eff} and nonpolar optic-phonon coupling constant D_tK determined by the semiempirical method mentioned in the text.

The probability of scattering caused by the AC processes can be expressed using the effective acoustic-mode deformation potential.[17] GaAs and GaP alloying has little effect on the shear deformation potential, thus introducing the possibility of simple interpolation.[18] The dilatation deformation potential, however, is very much affected, being related to changes in valence-band-edge energy caused by alloying. Under SVCA the dielectric band theory can well express this energy distance. The hole-NPO coupling constant D_tK (Ref. 19) was also determined using Wiley's expression.[16] LO-phonon energy $\hbar\omega_0$ was estimated, where only the nearest-neighbor atomic interaction (bond-stretching force) was taken into account, because differences in heteropolarity due to alloying hardly affect the LO-phonon energy under SVCA. By using those resulting elastic constants and LO-phonon energy, the deformation potential and coupling constants D_tK for the $GaAs_{1-x}P_x$ series were estimated (Fig. 3).

B. Alloy scattering

Alloy scattering in random solids is a major mechanism for carriers in mixed III-V alloys. Random atomic configuration or replacement of these alloys produces a "hill-and-valley" structure of the band edges. Therefore, the energy distance between "up" and "down" of the valence-band-edge is perhaps the better measure of the alloy-scattering potential. Dielectric band theory[13] produces a valence-band-edge energy of Γ_{15}^v. Then, the fluctuation of the valence-band-edge position can be quantitatively determined.

We investigated the relaxation time resulting from this type of alloy scattering.[5] These relaxation times, however, are much longer than the usual lattice scattering times, meaning that alloy scattering for holes is not dominant, and the reduction in hole mobility due to this kind of scattering will most likely be small.

IV. TRANSPORT COEFFICIENT

Experimental and theoretical values must be carefully compared to confirm a number of estimated fundamental material constants used in discussing electric transport phenomena. This section presents hole mobility results in III-V compounds and their semiconductor alloys. Results are first expressed in using the effective-relaxation-time approximation. When scattering is inelastic, no exact relaxation time exists, although this approximation can be useful within certain limits. However, the questionable estimation of scattering-in and -out fluxes for holes causes the failure of the simple effective-relaxation-time approximation, even at low temperature, because of the multivalence-band structure.

The mobility calculation method relies on the generally accepted fact that a great deal of analytical progress can be achieved by regarding scattering in terms of the Boltzmann equation. The explicit expression for the hole distribution function perturbed by small electric fields is obtained as linear, finite, coupled difference equations. Several scattering mechanisms are properly combined, and the mobility is calculated from the perturbed distribution function. According to Rode,[19,20] the present method avoids much of the purely mathematical detail necessary in the variational method, and is straightforward enough that the physical meaning of the results is clear. In fact, all of the advantages of the variational approach have been preserved. A set of coupled, linear finite difference equations can be written, which describes the hole distribution function under the influence of a weak electric field. These equations have been solved by numerical iteration.

A. Hole mobility: Effective-relaxation-time approximation (ERTA)

Total relaxation time was determined by taking into consideration the effects of both intra- and inter-valence-band transitions owing to the existence of the three types of holes. Hole mobility was then calculated[6,9] based on the four types of lattice scattering and the alloy-scattering processes. Figure 4 shows composition dependence of drift mobility for holes in $GaAs_{1-x}P_x$. At low temperature [Fig. 4(a)], acoustic-mode scattering exhibits dominance over optic scattering. Calculated mobility due to optic-mode scattering increases with composition x. When temperature increases, a drastic increment occurs in

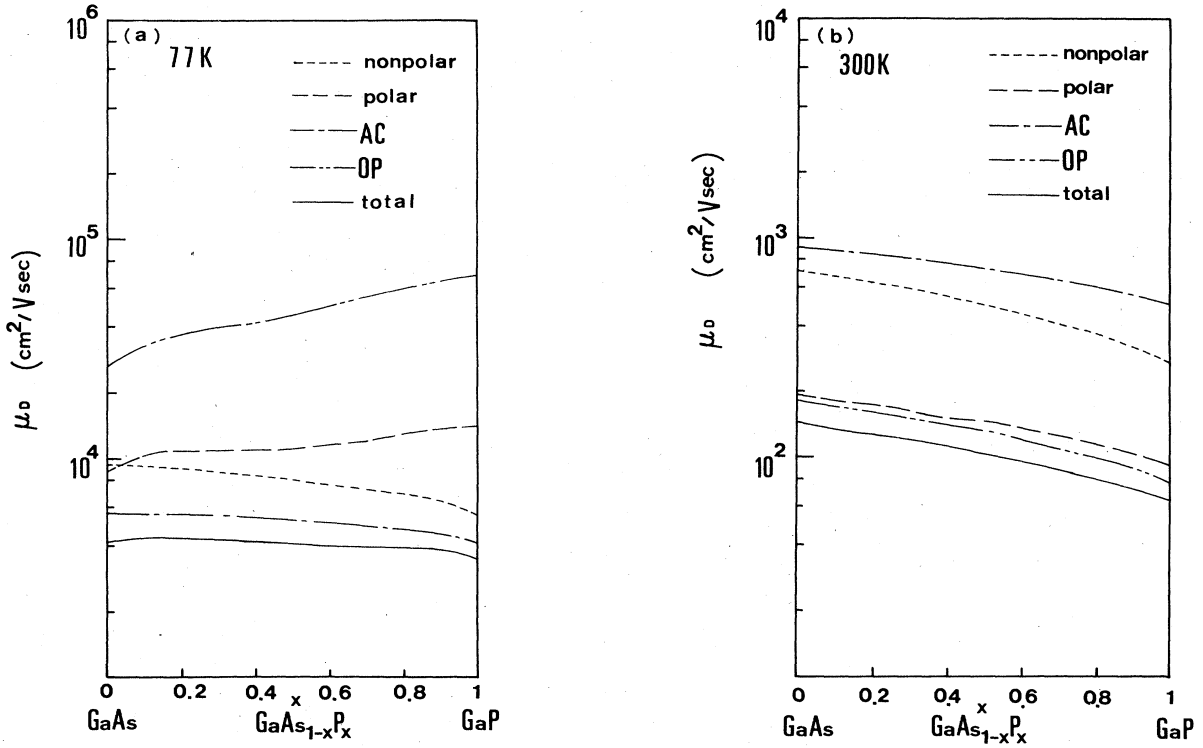

FIG. 4. Composition dependence of hole drift mobility in Ga-As-P at (a) 77 K and (b) 300 K by the effective-relaxation-time approximation (ERTA) method for the Kane model. Results noted for the acoustic-mode deformation-potential scattering (AC) mode include the influence of acoustic-mode lattice scattering [AC and piezoelectric scattering (PZ)]. Those noted for the optic-mode deformation-potential scattering (OP) mode include the influence of optic-mode lattice scattering [polar optic-phonon scattering (PO) and nonpolar optic-phonon scattering (NPO)]. Those noted for nonpolar include scattering by nonpolar mode (AC and NPO), and those for polar include those by polar mode (PO and PZ).

scattering probability due to inelastic scattering processes (NPO and PO). This causes the dominant optic-mode scattering to determine the total mobility [Fig. 4(b)].

B. Hole mobility: Difference approximation (DA)

While qualitative variations in mobility due to composition can be investigated by the effective-relaxation-time approximation, quantitative agreement is needed between theoretical and experimental results. Considerable discrepancy is expected between experimental data and calculated results (ERTA) because the relaxation-time concept must be abandoned over much of the temperature range of interest owing to the dominance of inelastic scattering. For the sake of a detailed comparison, attention has been focused on the results of pure III-V semiconductors (GaAs and GaP) due to the lack of experimental Ga-As-P—alloy system data. Theoretical hole mobilities are calculated using the convenient and accurate approach of Rode[19,20] and by solving the coupled Boltzmann equations directly.

Only two sub-valence-bands of heavy and light holes are considered. This simplification is valid for materials whose Δ_0 is comparably larger (GaAs), because in those materials the effect of split-off holes is considerably smaller.

Fluctuations in the distribution functions for heavy ($i=1$) and light ($i=2$) holes resulting from various scattering processes are given by

$$\left.\frac{\partial f_i}{\partial t}\right|_{\text{coll}} = -\frac{e\mathbf{E}}{\hbar}\cdot\nabla_{\mathbf{k}} f_i + \int d\mathbf{k}[s_{ii}(\mathbf{k}',\mathbf{k})f_i(\mathbf{k}') - s_{ii}(\mathbf{k},\mathbf{k}')f_i(\mathbf{k})] + \int d\mathbf{k}'[s_{ji}(\mathbf{k}',\mathbf{k})f_j(\mathbf{k}') - s_{ij}(\mathbf{k},\mathbf{k}')f_i(\mathbf{k})] \ , \tag{5}$$

in which inter- as well as intra-sub-valence-band transitions are taken into account. The second term is caused by intraband transitions and the third one by interband transitions. $\mathbf{E}$ is the electric field. $s_{ij}(\mathbf{k},\mathbf{k}')$ is the probability per unit time that an electron initially in the state characterized by $\mathbf{k}$ will make a transition into the state characterized by $\mathbf{k}'$. Scattering processes due to alloy scattering and four different lattice scattering mechanisms (AC, PZ, NPO, and PO) must be taken into account for the parameter $s(\mathbf{k},\mathbf{k}')$. Scattering is assumed to occur elastically due to acoustic-mode vibration (AC and PZ). Scattering due to optic-mode vibration (NPO and PO) is assumed to occur inelastically with an energy difference $\hbar\omega_0$ approximately equal to the LO-phonon energy at the center of the Brillouin zone (Sec. III A).

Application of an external electric field disturbs the carrier-distribution equilibrium. If the external field is weak enough, the following assumption holds:

$$f_i(\mathbf{k}) \sim f_i^0(k) + x g_i(k) \ , \tag{6}$$

where $k = |\mathbf{k}|$ and $x = \cos\xi$ is the cosine of the angle between the wave vector and the applied electric field. An induced drift current is entirely contained in perturbation distribution xg.

For a nondegenerate semiconductor, the Boltzmann equation relates g through the various scattering mechanisms to the electric field and f^0. According to Rode,[19,20] the resulting coupled Boltzmann equations are obtained as (Appendix A)

$$\frac{eE}{\hbar}\frac{\partial f_i^0}{\partial k} = g_i(\epsilon)\int d\mathbf{k}\left[s_{ii}^e(\mathbf{k}',\mathbf{k})\frac{x'}{x} - s_{ii}^e(\mathbf{k},\mathbf{k}') - s_{ii}^i(\mathbf{k},\mathbf{k}') - s_{ij}^e(\mathbf{k},\mathbf{k}') - s_{ij}^i(\mathbf{k},\mathbf{k}')\right] + g_j(\epsilon)\int d\mathbf{k}'\frac{x'}{x}s_{ji}^e(\mathbf{k}',\mathbf{k})$$
$$+ g_j(\epsilon^{\pm})\int d\mathbf{k}'\frac{x'}{x}s_{ii}^i(\mathbf{k}',\mathbf{k}) + g_j(\epsilon)\int d\mathbf{k}'\frac{x'}{x}s_{ji}^i(\mathbf{k}'\mathbf{k}) \quad (i\neq j) \ . \tag{7}$$

For convenience, s is divided into two terms to reflect elastic scattering s^e and inelastic scattering s^i. Representation wave number $\mathbf{k}$ is also changed to energy according to the ϵ-$\mathbf{k}$ dispersion relation (Sec. II). $\epsilon^{\pm}$ corresponds to the enhanced energy state due to optic-phonon absorption (ϵ^+) and the depleted state following emission (ϵ^-).

In order to obtain a conventional expression for the coupled Boltzmann equations, a scattering rate S_{ij} is introduced and defined by

$$S_{ij}^e = \int d\mathbf{k}' s_{ij}^e(\mathbf{k},\mathbf{k}') \ . \tag{8}$$

The transition probability s_{ij} is composed of two terms of the transition matrix and the density of states. Moreover, the transition matrix M_{ij} is also determined by two terms of the symmetry properties of the carrier wave function and the perturbed potential when the perturbing potential is not so strongly dependent on the band structure.[21] The former term is called the overlap function G_{ij}.[22] It is necessary to distinguish an anisotropy of scattering between intra-valence-band transitions and inter-valence-band transitions because of the complicated multi-valence-band structure. This distinction can be carried on by multiplying an overlap function G_{ij} by the corresponding Fourier component of the scattering potential, since both the intra- and inter-valence-band transitions occur with small change of wave vectors.[21,22] In calculation we represent the anisotropy of scattering due to the symmetry properties of the wave function of Bloch holes by the following overlap function G_{ij}:[21]

$$G_{ii}=\tfrac{1}{4}(1+\cos^2\xi)=\tfrac{1}{4}(1+x^2)\ ,$$
$$G_{ij}=\tfrac{3}{4}\sin^2\xi=\tfrac{3}{4}(1-x^2)\ , \tag{9}$$

in which the k dependence of G_{ij} is approximately neglected. We consider, however, the anisotropy and nonparabolicity of the valence band carefully in the integration to obtain the scattering rate.

Consequently, the resulting coupled Boltzmann equations are reduced to

$$g_i=\frac{g_j(\epsilon)\tilde{S}^e_{ji}+\sum_{\pm}g_j(\epsilon^{\pm})\tilde{S}^i_{ii}+\sum_{\pm}g_j(\epsilon^{\pm})\tilde{S}^i_{ji}-(eE/\hbar)\dfrac{\partial f^0_i}{\partial k}}{S^e_{ii}+S^i_{ii}+S^e_{ij}+S^i_{ij}-\tilde{S}^e_{ii}}$$

with

$$\tilde{S}^e_{ij}=\int d\mathbf{k}'\frac{x'}{x}s^e_{ij}(\mathbf{k}',\mathbf{k})\ , \tag{10}$$

where the superscripts e and i of S_{ij} correspond to elastic

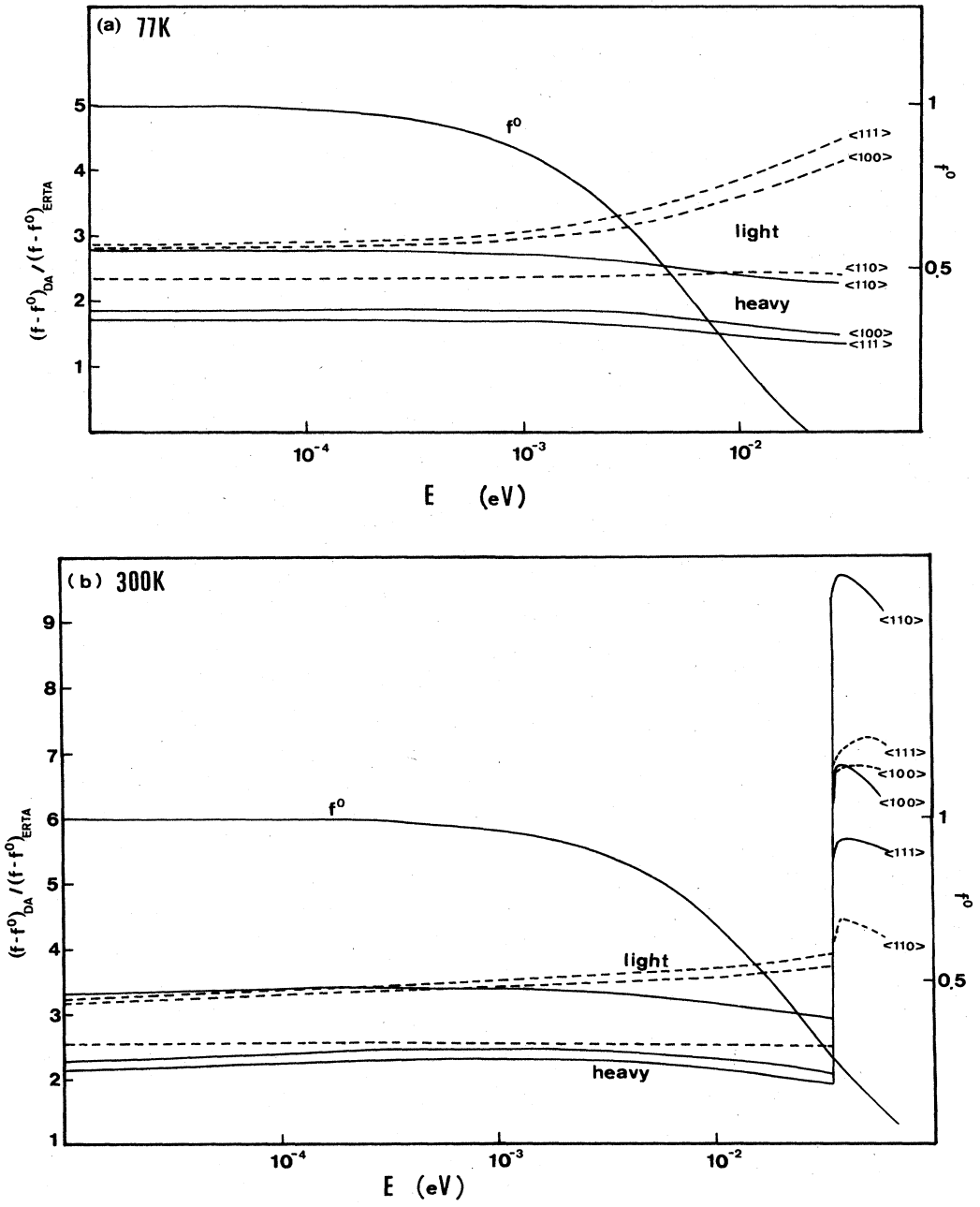

FIG. 5. Energy dependence of ratio $(f-f^0)_{DA}/(f-f^0)_{ERTA}$ for heavy (solid line) and light (dashed line) holes at (a) 77 K and (b) 300 K. $\langle ijk\rangle$ is the initial wave-vector direction. The nonperturbed Fermi-Dirac distribution function f^0, which is normalized through multiplication by $e^{-\eta}$, where η is Fermi energy, is also shown.

and inelastic scattering, respectively. The function g_i depends on the initial state $(\epsilon_i,\theta_i,\phi_i)$. Numerical solutions for these coupled Boltzmann equations can be obtained by iteration. The inter-valence-band interaction must be taken into account in the scattering rate using the density of states.

ERTA validity is first investigated. The difference of the distribution function from its equilibrium value for the DA approach can be obtained from calculations of Eq. (10). The corresponding difference of the distribution function for the ERTA approach is formally given in terms of an effective relaxation time as follows:

$$(f-f^0)_{\rm ERTA}=-\tau^T\frac{e\mathbf{E}}{\hbar}\cdot\nabla_{\mathbf{k}}f\ , \tag{11}$$

where τ^T is the total relaxation time. By comparing the values of $(f-f^0)_{\rm DA}$ and $(f-f^0)_{\rm ERTA}$ the validity of ERTA can be discussed.

Although the concept of the "relaxation-time" approximation is inconsistent in inelastic scattering processes, this approach has been applied to those processes by using a conventional expression as the inelastic relaxation time, in which the effect of the inelasticity is taken into account with the energy increase and decrease. Therefore, the total relaxation time in Eq. (11) is

$$\frac{1}{\tau^T(\epsilon)}=\frac{1}{\tau^e(\epsilon)}+\frac{1}{\tau^i(\epsilon\pm\Delta\epsilon)}\ , \tag{12}$$

where τ^e and τ^i are the relaxation times in the elastic and inelastic scattering processes, respectively. Since the valence band is composed of several subbands, each relaxation time τ^j ($j=e$ and i) should be determined from a summation over the subbands as

$$\frac{1}{\tau^j}=\sum_n\frac{1}{\tau_n^j} \tag{13}$$

(in simple ERTA). Subscript n means the nth subband. The relaxation time τ_n^j is proportional to the density of states of the nth subband (d_n). Mixing the various scattering processes described in Sec. III, we have calculated the ratio of $(f-f^0)_{\rm DA}/(f-f^0)_{\rm ERTA}$ for heavy and light holes.

In the low-temperature and low-energy states [Fig. 5(a)] in which elastic scattering due to acoustic-mode vibration is dominant, the ratios show almost energy-independent values. The values are also comparatively unity. The initial-state dependence is not so significant for both heavy and light holes because the occupied equienergy surfaces at low energy (i.e., low temperature) are not so strongly anisotropic. The ratio for light holes is larger

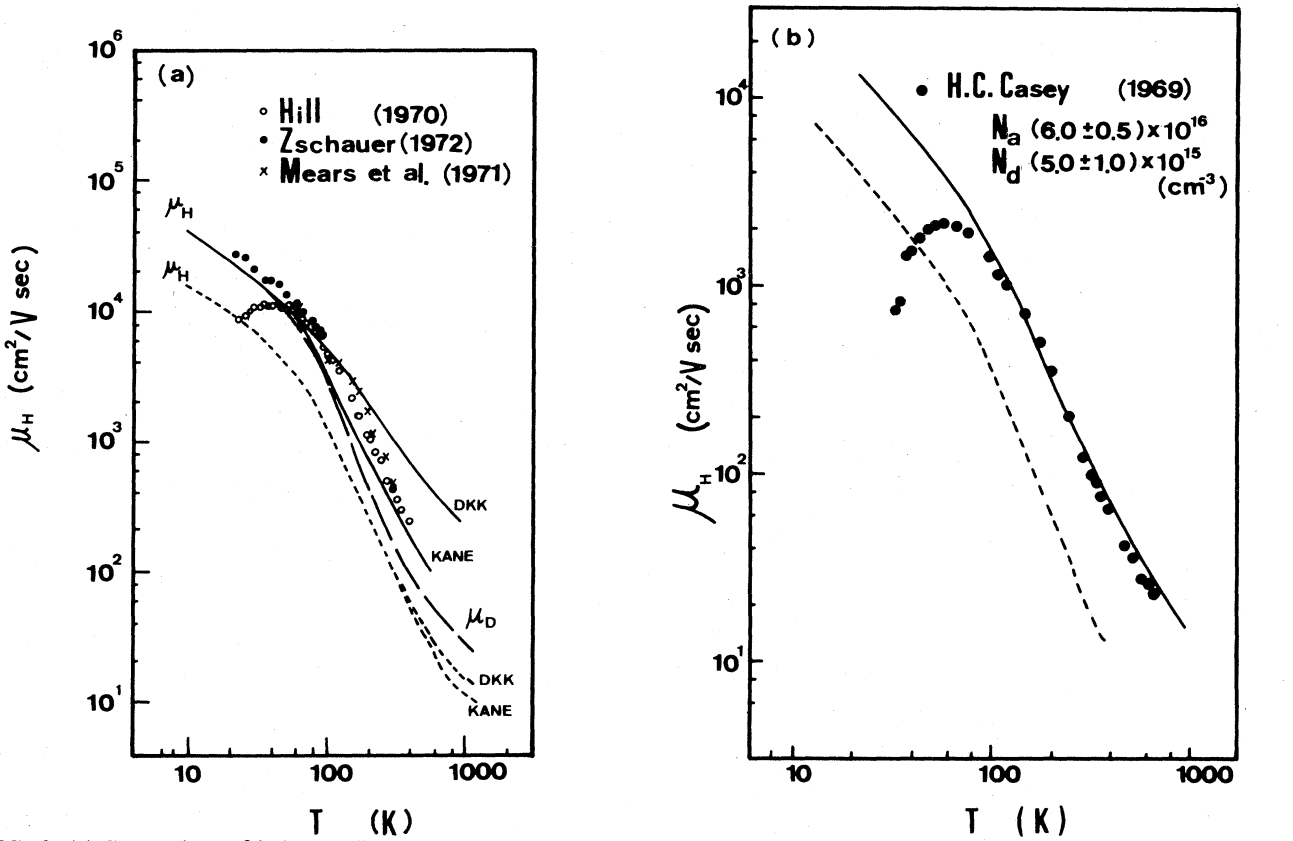

FIG. 6. (a) Comparison of hole mobility between theoretical results and experimental ones for GaAs (Ref. 23). Solid line gives results of the hole mobility of the difference approximation (DA) method and broken line of the ERTA method. Inter-valence-band interaction can be seen by comparing theoretical results for the Kane and DKK band models. μ_H and μ_D signify the Hall mobility and the drift mobility (DA), respectively. (b) Comparison of hole mobility between theoretical results and experimental ones for GaP (Ref. 24). A slight parameter adjustment in $\Xi_{\rm eff}$ and D_tK (about 10% from those estimated in Sec. III A) has been made. Symbols N_a and N_d are the impurity density of acceptors and donors, respectively.

than that for heavy holes since the density of states for light holes is smaller than that for heavy holes. This is consistent with the physical view of the "light" holes being more mobile than the "heavy" holes.

In the high-temperature and high-energy states [Fig. 5(b)] in which elastic scattering due to optic phonons is dominant, the values of the ratio for both heavy and light holes are greatly different from unity. A steep and large increase of ratios can be found when inelastic scattering occurs ($\hbar\omega_0 = 35$ meV). These steep increases play an effective role in the determination of mobility because of a broadened distribution function f^0 at high temperature.

Figure 6(a) shows the resulting hole mobility of GaAs reestimated using the DA method. The ambiguity of scattering-in and scattering-out processes in ERTA makes the value of g' smaller than that of g using DA (Appendix B). This causes an underestimation of the theoretical mobility. Better agreement between theoretical (DA) and experimental results can be found.

By using the expression[22] usually quoted for the polar optic-phonon-mode mobility, DiDomenico[25] systematically discussed carrier mobility in three typical types of semiconductors and concluded that scattering from PO modes is not dominant for holes in the higher-temperature region. However, parameter-fitting treatment is necessary in order to find an agreement between their theoretical results and experiments, because changes in wave vectors due to inelastic scattering are neglected. On the contrary, if the DA approach is employed and the inelastic scattering processes as well as the complication of the valence-band structure are carefully taken into consideration, an excellent agreement can be found without fitting parameters.

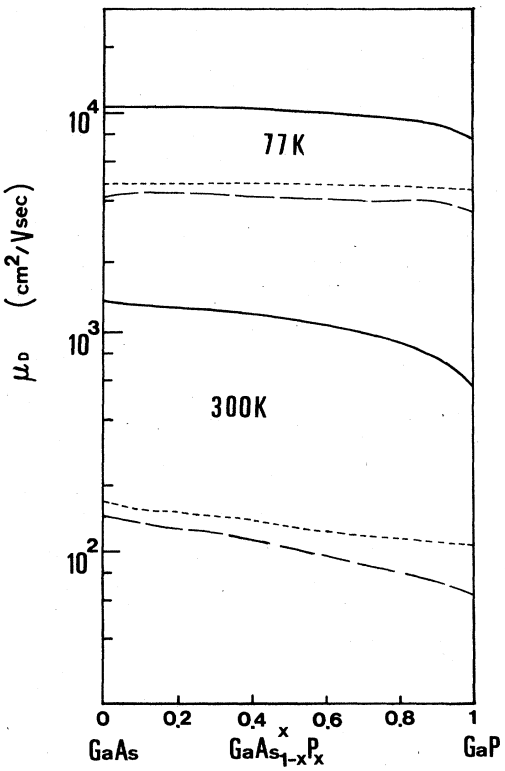

FIG. 7. Resulting hole drift mobility for $GaAs_{1-x}P_x$ in response to total lattice scattering (AC, PZ, NPO, and PO) and alloy scattering, with varying P concentration. Solid line shows the results by the DA method for the Kane band model. Long-dashed lines and short-dashed lines represent those by the ERTA applied to the Kane and the DKK model, respectively.

Two typical disagreements are found at low and high temperature. These are interpreted as follows. When the temperature increases, the occupation probability in the third valence band (split-off holes) increases. The inter- and intra-sub-valence-band transition relating to this subband should be carefully considered as this causes a reduction in the total scattering ratio. Neglecting the split-off holes results in an overestimation of hole mobility in the higher temperature region. These disagreements caused by neglecting the split-off holes are strengthened in GaP because of the smaller value of its split-off energy [Fig. 6(b)]. There is another ambiguity in that we used here Wiley's approximate formula for the overlap function G_{ij}, in which the k dependence is neglected. This expression is valid only for the top energy state, which is inconsistent in the higher-temperature region. The disagreement, which appeared at low temperatures, is caused by the neglect of impurity scattering.

Figure 7 shows a composition dependence of drift mobility for holes in $GaAs_{1-x}P_x$. When the temperature increases, the difference between results from DA and those from ERTA is enhanced because of the increment of inelastic processes (PO and NPO). The effect of the inter-valence-band interaction appears as a reduction of mobility in all compositions. The magnitude of this effect increases with P content or with temperature.

V. CONCLUSION

In conclusion:

(1) Valence-band parameters and coupling constants for $GaAs_{1-x}P_x$ alloys have been semiempirically estimated. Alloy-scattering potentials for holes in such alloys have also been obtained by extending the dielectric band method.

(2) The inter-valence-band interaction is strengthened with an increase of P content, because of a split-off energy reduction.

(3) Theoretical hole-transport coefficients agree better with experimental results when the coupled Boltzmann equations are solved using the differential approach. The multisubband structure for the valence band breaks the simple relaxation-time-approximation approach for holes, even at low temperatures.

ACKNOWLEDGMENTS

The authors would like to give emphatic thanks to Dr. Kenji Kumabe and Dr. Takeshi Toriyama for their helpful discussions. The authors from Keio University would like to thank the Takeda Science Foundation for financial support. One of the authors (K.T.) would like to express special thanks to Dr. Koji Sakui for his encouragement throughout this work.

APPENDIX A

Substituting Eq. (6) into (5), the coupled Boltzmann equation is rewritten as

$$\frac{e\mathbf{E}}{\hbar}\cdot\nabla_{\mathbf{k}} f_i = \int d\mathbf{k}'[s_{ii}(\mathbf{k}',\mathbf{k})f_i^0(\mathbf{k}')-s_{ii}(\mathbf{k},\mathbf{k}')f_i^0(\mathbf{k})] + \int d\mathbf{k}'[s_{ii}(\mathbf{k}',\mathbf{k})x'g_i(\mathbf{k}')-s_{ii}(\mathbf{k},\mathbf{k}')xg_i(\mathbf{k})] + \int d\mathbf{k}'[s_{ji}(\mathbf{k}',\mathbf{k})f_j^0(\mathbf{k}')-s_{ij}(\mathbf{k},\mathbf{k}')f_i^0(\mathbf{k})] + \int d\mathbf{k}'[s_{ji}(\mathbf{k}',\mathbf{k})x'g_j(\mathbf{k}')-s_{ij}(\mathbf{k},\mathbf{k}')xg_i(\mathbf{k})] . \tag{A1}$$

When the electric field is assumed to be applied along z direction $\mathbf{E}=(0,0,E)$, which does not lose generality, the left side of Eq. (A1) is

$$\frac{e\mathbf{E}}{\hbar}\cdot\nabla_{\mathbf{k}} f_i = \frac{e}{\hbar}E\left[(\cos\xi)\frac{\partial f_i^0}{\partial k}+(\cos^2\xi)\frac{\partial g}{\partial k}+\frac{\sin^2\xi}{k}g\right] . \tag{A2}$$

Following Rode, multiplication of Eq. (A1) by unity, the zeroth-order Legendre polynomial and integration over $x=\cos\xi$ yields

$$x\frac{eE}{\hbar}\frac{\partial f_i^0}{\partial k} = \int d\mathbf{k}'[s_{ii}(\mathbf{k}',\mathbf{k})x'g(\mathbf{k}')-s_{ii}(\mathbf{k},\mathbf{k}')xg(\mathbf{k})] + \int d\mathbf{k}'[s_{ji}(\mathbf{k}',\mathbf{k})x'g(\mathbf{k}')-s_{ij}(\mathbf{k},\mathbf{k}')xg(\mathbf{k})] . \tag{A3}$$

Distinguishing the scattering processes by s_{ij}^e (elastic process) and s_{ij}^i (inelastic process), Eq. (A3) is rewritten as

$$\frac{eE}{\hbar}\frac{\partial f_i^0}{\partial k} = \frac{\int d\mathbf{k}'[s_{ii}^e(\mathbf{k}',\mathbf{k})x'g_i(\mathbf{k}')+s_{ii}^i(\mathbf{k}',\mathbf{k})x'g_i(\mathbf{k}')]}{x} - g_i(k)\int d\mathbf{k}'[s_{ii}^e(\mathbf{k},\mathbf{k}')+s_{ii}^i(\mathbf{k},\mathbf{k}')] + \frac{\int d\mathbf{k}'[s_{ji}^e(\mathbf{k}',\mathbf{k})x'g_j(\mathbf{k}')+s_{ji}^i(\mathbf{k}',\mathbf{k})x'g_j(\mathbf{k}')]}{x} - g_i(k)\int d\mathbf{k}'[s_{ij}^e(\mathbf{k},\mathbf{k}')+s_{ij}^i(\mathbf{k},\mathbf{k}')] . \tag{A4}$$

As the integration is carried on over the final states, $g_i(k')$ can be approximately treated as follows. Since the carriers are scattered into the equienergy surfaces by an elastic process, changes in wave vectors due to both intra- and inter-valence-band transitions are comparatively small. Thus, those integrations appearing in elastic scattering can be carried on, neglecting the change in wave vectors. On the other hand, those integrations appearing in inelastic scattering can be performed by adding (phonon absorption) or subtracting (phonon emission) a characteristic energy equal to LO-phonon energy. Thus, the corresponding final states should be modified from $\mathbf{k}'$ to $\mathbf{k}'^{\pm}$. Then resulting coupled Boltzmann equations are obtained as in the text.

APPENDIX B

A slight difference in the ratio from unity can be found for holes even at low temperature (77 K), in which elastic scattering is thought to be dominant. It is said that when the scattering is mainly elastic, the simple ERTA ($S_{\mathbf{k},\mathbf{k}'}=S_{\mathbf{k}',\mathbf{k}}$) is proper to describe such scattering processes in a single band. The discrepancy for holes is caused by the multisubband structure of the valence band as follows.

Taking into account only elastic scattering, the difference $(f-f^0)_{\mathrm{DA}}$ is determined from the following g_i^e (e refers to elastic as before):

$$g_i^e = \frac{g_i(\epsilon)\tilde{S}_{ij}^e-(eE/\hbar)(\partial f_i^0/\partial k)}{S_{ii}^e+S_{ij}^e-\tilde{S}_{ii}^e} . \tag{B1}$$

The corresponding difference in $(f-f^0)_{\mathrm{ERTA}}$ is given by using the elastic scattering relaxation time τ^e as

$$(f-f^0)_{\mathrm{ERTA}}^e\,|_i = -\tau_T^e\frac{e\mathbf{E}}{\hbar}\cdot\nabla_{\mathbf{k}} f \tag{B2}$$

with

$$1/\tau_T^e = 1/\tau_i^e + 1/\tau_j^e \quad (i\neq j) .$$

While the $(f-f^0)_{\mathrm{ERTA}}$ deduced from the simple ERTA is formally determined only by the initial subband, the final subband as well as initial subband should be considered when the DA is used to solve the coupled Boltzmann equation. This is because the scattering-in and scattering-out fluxes[20] between the different subbands are taken into consideration when the DA approach is employed. Therefore, the additional terms necessitated by the intersubband transition should be strictly taken into account if the carriers occupy the multisubbands, i.e., the valence band. On the contrary, carriers occupy the single band (electron), no intersubband transition results in $s_{ij}=0$. For electrons this guarantees strictly the validity of ERTA in the elastic scattering processes.

---

*Permanent address: Musashino Electrical Communication Laboratory.

[1]N. A. Goryunova, F. P. Keasmnly and D. A. Nasledov, in *Semiconductors and Semimetals,* edited by R. K. Willardson and A. C. Beer (Academic, New York, 1968), Vol. 4, Chap. 7.

[2]G. Dresselhaus, A. F. Kip, and C. Kittel Phys. Rev. **98**, 368 (1955).

[3]E. O. Kane, in *Semiconductors and Semimetals,* Ref. 1, Vol. 1, Chap. 3.

[4]B. R. Nag, *Electron Transport in Compound Semiconductors* (Springer, Berlin, 1980).

[5]K. Takeda and N. Matsumoto, J. Phys. C **17**, 5001 (1984).

[6]K. Takeda, K. Sakui, A. Taguchi, and M. Sakata, J. Phys. C **16**, 792 (1983).

[7]G. Dresselhaus, Phys. Rev. **100**, 580 (1955).

[8]M. Asche and C. von Borzeskowski, Phys. Status Solidi **37**, 433

(1970).
[9]K. Takeda, A. Taguchi, and M. Sakata, J. Phys. C **16**, 2237 (1983).
[10]P. Lawaetz, Phys. Rev. B **4**, 3460 (1971).
[11]A. G. Thompson, M. Cardona, K. L. Shaklee, and J. C. Wooley, Phys. Rev. **146**, 601 (1966).
[12]J. C. Phillips, Rev. Mod. Phys. **42**, 317 (1970).
[13]J. V. Van Vechten, Phys. Rev. **182**, 891 (1966); **187**, 1007 (1969).
[14]K. Takeda, Y. Maeda, E. Ohta, M. Sakata, G. Kido, and N. Miura, Phys. Status Solidi B **115**, 369 (1983).
[15]R. W. Keyes, J. Appl. Phys. **33**, 3371 (1962).
[16]J. D. Wiley, Solid State Commun. **8**, 1865 (1970).
[17]P. Lawaetz, Phys. Rev. **174**, 867 (1968).
[18]T. Soma, Phys. Status Solidi B **110**, K167 (1982).
[19]M. Costato, G. Gaggliani, C. Jacoboni, and L. Reggiani, J. Phys. Chem. Solids **35**, 1605 (1974).
[20]D. L. Rode, Phys. Rev. B **2**, 1012 (1970); D. L. Rode and S. Knight, *ibid.* **3**, 2534 (1971).
[21]J. D. Wiley, Phys. Rev. B **4**, 2485 (1971).
[22]H. Ehrenreich, J. Phys. Chem. Solids **8**, 130 (1959).
[23]D. E. Hill, J. Appl. Phys. **41**, 1815 (1970); K. H. Zschauser, in *Proceedings of the Fourth International Symposium of GaAs and Related Compounds, Boulder, Colorado, 1972,* edited by C. Hilsum, Conference Series No. 17 (Wright, London, 1972); A. L. Mears and R. A. Stradling, J. Phys. C. **4**, L22 (1972).
[24]H. C. Casey, J. Appl. Phys. **40**, 2945 (1969).
[25]J. D. Wiley and M. DiDomenico, Jr., Phys. Rev. B **2**, 427 (1970).